Physics-Inspired Machine Learning for Radiomap Estimation: Integration of Radio Propagation Models and Artificial Intelligence

Songyang Zhang, Member, IEEE, Brian Choi, Senior Member, IEEE, Feng Ouyang, Senior Member, IEEE, Zhi Ding, Fellow, IEEE

Abstract—Radiomap captures geometrical distribution of radio frequency signal power. As an important tool to qualitatively and quantitatively describe radio propagation behavior and spectrum occupancy, radiomap has found broad applications in deployment and configuration of modern wireless and Internetof-Things networks. Practically, a high-resolution radiomap can be reconstructed from partial or sparse observations collected by mobile devices or sensors. To leverage the power of radiomap, efficient radiomap reconstruction from sparse samples has emerged as an urgent challenge. To capture both the underlying data statistics and estimate the physical radio frequency models, this work introduces three types of physics-inspired machine learning approaches to radiomap reconstruction. The experimental results demonstrate the potentials of integrating data-driven artificial intelligence with model-based radio propagation behavior for radiomap reconstruction.

Index Terms—Radiomap estimation, machine learning, radio propagation models

I. INTRODUCTION

Tremendous progresses in information technologies have stimulated numerous novel concepts and advanced wireless technologies, such as Internet-of-Things (IoT), 3GPP's 5G terrestrial and non-terrestrial network (NTN) services, and modern emergency communication systems. For these wireless applications, efficient network coverage analysis is critical to spectrum efficiency and quality-of-service (QoS). A vital tool to capture spectrum coverage is the radio strength distribution in spatial domain for various spectrum bands of concern, known as radiomap (or radio environmental map) [1]. As shown in Fig. 1, radiomap generally refers to an image that represents the geometrical signal power spectrum density (PSD) [2], resulting from concurrent wireless signal transmissions. In a radiomap, the PSD can be a function of position, frequency and time [3]. Enriching information on radio propagation and spectrum occupancy, radiomap has assisted and inspired a rich plethora of applications, such as outage detection, unmanned aerial vehicle (UAV) path planning, and landscape information reconstruction [4].

In practical scenarios, dense radiomap is usually estimated from sparse observations collected by sensors, driving tests, or user devices [5]. An example of spectrum management for a hybrid satellite-terrestrial network assisted by radiomap is shown as Fig. 1, where different tasks, such as beam planning and system fault diagnosis, can leverage the estimated dense radiomap from sparse measurements. Thus, to utilize the power of radiomap in network optimization and spectrum resource allocation, fine-resolution radiomap estimation (RME) from sparse or partial observations is a critical problem in modern wireless networking.

Most existing methods of radiomap estimation can be categorized into either model-based or learning-based methods. Model-based methods usually assume specific functions of radio propagation, such as log-distance path loss model (LDPL) [6] and inverse distance weighted (IDW) [7]. However, inappropriate utilization of the radio propagation models may limit the accuracy of model-based RME. For example, in complex environments, the radio power distribution is more sensitive to surrounding landscape information, with which the propagation models cannot efficiently capture. Efficient models for interference and shadowing effects are always challenging in realistic scenarios. Alternatively, learning-based approaches do not assume a specific model but leverage more surrounding information. Typical examples include the RadioUnet [8], auto-encoder [9] and conditional generative adversarial nets [10], where deep learning approaches are applied to characterize the underlying data statistics of observed PSD samples for radiomap estimation. Despite some successes, deep learning-based methods rely heavily on the quality and quantity of observations and training data. In many realistic scenarios, training data are often inadequate in size and sometimes non-uniformly distributed geometrically. Furthermore, samples in different training sets do not necessarily fit the same radio propagation models and parameters. The robustness and generalization of data-driven approaches for radiomap estimation remain elusive.

To fully utilize the statistical data distributions and physical radio propagation model, this article introduces physics-inspired machine learning for radiomap estimation in modern wireless communications systems, taking advantages from both model-based and learning-based approaches. Specifically, we first introduce various categories of radiomap estimation and give an overview of existing RME frameworks. We next introduce three different types of physics-inspired machine

S. Zhang is with Department of Electrical and Computer Engineering, University of Louisiana at Lafayette, Lafayette, LA, 70504. (E-mail: songyang.zhang@louisiana.edu).

Z. Ding is with Department of Electrical and Computer Engineering, University of California at Davis, Davis, CA, 95616. (E-mail: zd-ing@ucdavis.edu).

B. Choi and F, Ouyang are with Johns Hopkins University Applied Physics Laboratory, Laurel, Maryland, USA, 20723. (E-mail: {Brian.Choi, Feng.Ouyang}@jhuapl.edu).

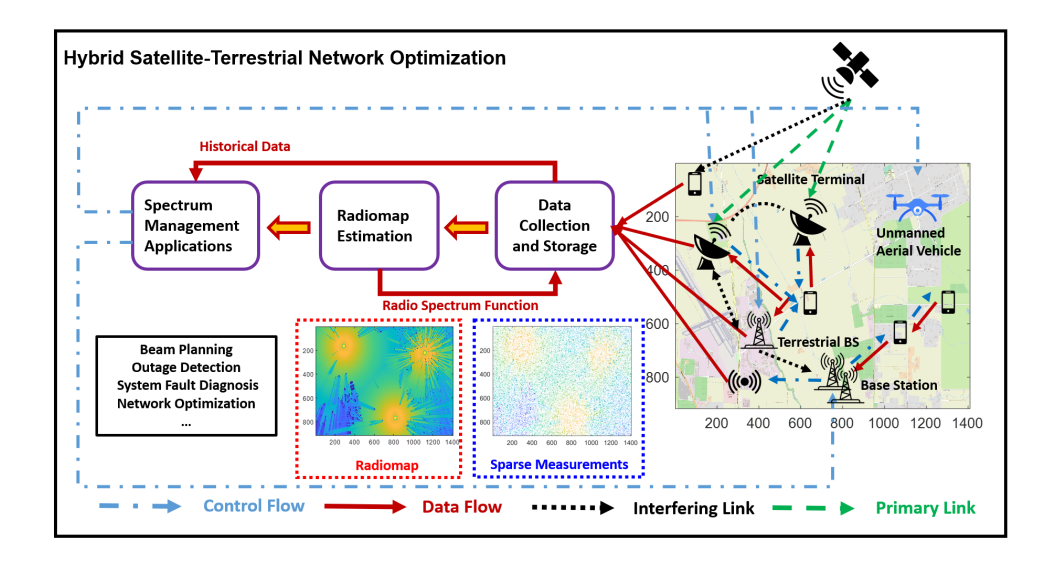


Fig. 1. Example of Radiomap-Assisted Network Optimization in Satellite-Terrestrial Communications: Collecting samples of spectrum measurement from deployed sensors, a sparse radiomap (in blue block) is obtained, based on which a dense radiomap (in red block) is estimated for spectrum management tasks, such as beam planning, outage detection and system diagnosis.

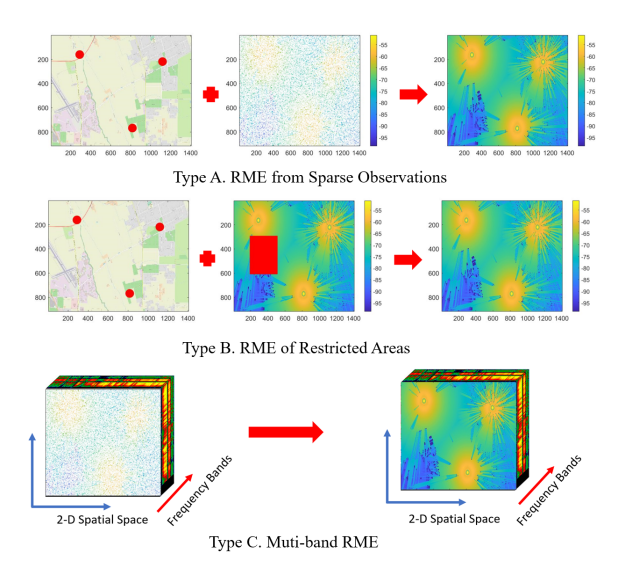


Fig. 2. Different Types of Radiomap Estimation: The first type of RME aims to estimate the dense radiomap from sparsely sampled observations, landscape information and position of transmitters; The second type shall inpaint the missing areas (in red) in a radiomap, given the surrounding environment and spectrum information; The multi-based RME reconstructs the radiomap given the PSD in multiple frequency bands.

learning infrastructures for efficient radiomap estimation. Finally, we summarize our findings, highlight current challenges, and identify research opportunities in radiomap estimation and RME-assisted spectrum management.

II. RADIOMAP ESTIMATION: FORMULATION AND CHALLENGES

A. Problem Description

Describing the spatial distribution of signal power in various spectral bands, a radiomap is usually characterized by the PSD, which is a function of location \mathbf{z} , frequency f, and sometimes with time t, denoted by $r(\mathbf{z}, f, t)$. Since a radiomap can be

dynamically reconstructed from real-time measurements for different time periods, we mainly focus on RME in a specific time window, which can be generalized into different time slots. Here, the location \mathbf{z} can be either a two-dimensional (2D) or three-dimensional (3D) vector depending on applications. Since the temporal properties of a radiomap depend on the system dynamics and can be resolved by the analysis at a certain time interval, most existing radiomap estimates average over time t and focus on $r(\mathbf{z}, f)$. This article shall focus on the RME of a region $\mathcal Z$ with frequency bands $\mathcal F$, i.e., $R(\mathcal Z, \mathcal F)$ consisting of all the PSD values $r(\mathbf{z}_i, f)$, where $\mathbf{z}_i \in \mathcal Z$ and $f \in \mathcal F$.

In practical scenarios, a dense (full) radiomap $R(\mathcal{Z},f)$ shall be estimated from sparse observations $\{r(\mathbf{z}_{o_i},f_{o_i})\}_{i=1}^M$, collected from user devices or sensors. Sparsity may manifest in frequency and space. Let the locations and frequencies of observations be denoted by \mathcal{Z}_o consisting of $\{\mathbf{z}_{o1},\mathbf{z}_{o2},\cdots,\mathbf{z}_{oM}\}$ and \mathcal{F}_o consisting of $\{f_{o1},f_{o2},\cdots,f_{oM}\}$, respectively. The general formulation of RME is to find a function $g(\cdot)$, i.e.,

$$\hat{R}(\mathcal{Z}, \mathcal{F}) = g(\mathcal{X}, R(\mathcal{Z}_o, \mathcal{F}_o)), \tag{1}$$

where \mathcal{X} is the environment information, such as urban map or building distribution. In practice, one may also focus on the RME at a single frequency f, which aims to find $\hat{R}(\mathcal{Z})$.

B. Categories of Radiomap Estimation

For an overview of RME, we first introduce the different categories of RME frameworks based on observation types, availability of data samples, and design of mapping function.

- 1) RME Categories According to Observation Types: Depending on observation types, some common RME cases shall fall into the following categories as shown in Fig. 2:
 - RME from sparse observations in single-frequency: This is the basic RME formulation, where the dense radiomap

is estimated by sparse observations from sensors. As illustrated in Type-A of Fig. 2, RME from observations in the same spectral band aims to uncover the spatial correlations to capture the radio propagation behavior and shadowing effects to reconstruct the radiomap at a specific frequency.

- RME for blank areas: In some scenarios, the restricted regions, such as mountain ranges or private properties, are inaccessible to radiomap measurements because of physical constraints or security consideration, leaving a blank areas in the radiomap shown as Type-B in Fig. 2. Unlike sparse observations, radio coverage in these areas is usually more sensitive to landscapes instead of following a classic radio propagation model. Considering the complicated surrounding environment, modelbased methods are less effective in this scenario. On the other hand, irregular measurement and blank areas on a radiomap can lead to less dependable RF power estimates in the objective regions, which further limits the efficacy of data-driven approaches [3]. Choice of efficient methodology for RME in missing areas remains an open research question.
- Multiband RME: Shown as Type-C in Fig. 2, Multi-band RME (MB-RME) is generalization of single-band RME characterized by Eq. (1). Beyond intra-spectrum spatial correlations, MB-RME can also describe inter-spectrum interference to provide a more accurate estimation.
- 2) Categorized by Available Radio Data: RME can be also categorized into interpolation-based RME and prediction-based RME, according to the number of available radiomaps:
 - Interpolation-based RME: Interpolation-based RME aims to estimate the missing values in one radiomap at a frequency f from the observed samples in the same region. Interpolation-based RME focuses on characterizing model parameters or data statistics for radiomap estimation in a single region \mathcal{Z} . Typical examples include the LDPL-based interpolation [6] and inverse weight (IDW) interpolation [7].
 - Prediction-based RME: Prediction-based RME usually relies on a set of radiomaps as training data to learn the mapping function $g(\cdot)$ from partial or sparse observations, together with landscape information and transmitter position, to the dense radiomap. Usually, sparse observations are sampled from the known radiomaps, together with the corresponding geometric features \mathcal{X}_k , as the input features. Given a set of training data samples of input features and output groundtruth dense radiomap, the mapping function $g(\cdot)$ can be learned for the estimation of testing radiomaps.
 - 3) Categorized by Mapping Function $q(\cdot)$:
 - Model-based RME: Model-based methods usually assume a radio propagation model for radio PSD loss, in terms of receiver and transmitter locations, such as LDPL or IDW [2], where the $g(\cdot)$ function follows a given model with unknown parameters estimated by minimizing error between observations and predictions. Since the performances of model-based methods rely on the

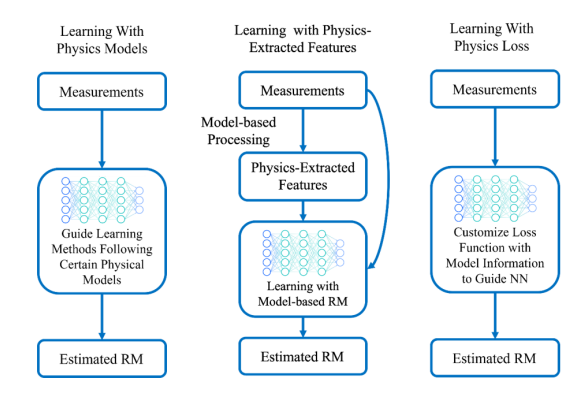


Fig. 3. Different Types of Physics-Inspired Machine Learning: The measurement includes the sparse observations collected by sensors, urban map scanned/segmented from satellite images, locations of transmitters, and other related features collected by integrated sensing and communication systems.

- functional approximation properties of model to fit the current radiomap and propagation behavior, it usually has a superior performance in smooth, regular environment while failing in complicated, irregular regions.
- Model-free RME: Model-free methods express the PSD at a particular location directly as a function of observations without a given radio propagation model. Here, the function $g(\cdot)$ can be designed as non-linear functions, such as neural networks [1], or solved by optimization problems, such as tensor completion [2]. Given complex formulation of model-free function $g(\cdot)$, sufficient observations are required to estimate the parameters of $g(\cdot)$ efficiently to overcome problems that arise from low-fidelity training data samples.

III. PHYSICS-INSPIRED MACHINE LEARNING FOR RME

Despite reported successes of purely model-based and learning-based RME approaches, model-based RME fails to capture surrounding landscape features and shadowing effects, while the learning-based RME tends to suffer from low-quality and insufficient training samples. It is critical to investigate new ways of developing radio physics inspired learning frameworks by utilizing radio propagation models and real-time radio measurements, coupled with landscape maps and satellite images, in order to generate radiomap of desired resolution. The emerging fields of physics-embedded machine learning hold the potential to address such challenges [11]. In this article, we introduce three different types of physics-inspired machine learning as shown in Fig. 3.

A. Learning with Physics-Extracted Features

The first type of physics-inspired machine learning is to extract physical features, as shown in Fig. 3. Generally, this type of RME consists of two steps: 1) process input data via feature extraction approaches based on radio propagation model; and 2) input the processed feature to the learning machines to estimate the $\hat{R}(\mathcal{Z}, \mathcal{F})$. The key for this kind of physics-inspired RME is to select suitable radio model and analytical tools for data pre-processing.

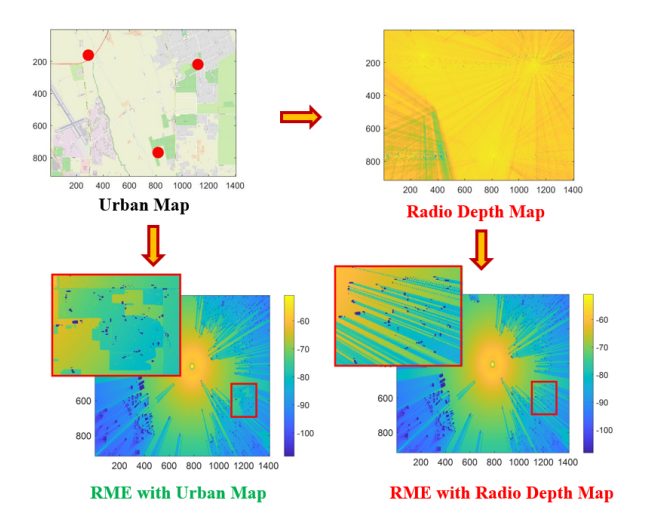


Fig. 4. Exemplary Results of RME (dBm) with Physics-Extracted Features (buildings are masked as blue): RME with Urban Map utilizes the environment map directly as the input for neural networks (MSE: 25.17); RME with Radio Depth Map uses the radio depth map as input (MSE: 8.74). IDW is used to generate the radio depth map.

Conventional model-based preprocessing applies model-based interpolation (MBI) to generate a rough estimation of PSD distribution, such as LDPL models and IDW models [2]. Then, the new input features of data samples for the training of neural network $g(\cdot)$ consists of the original and MBI-estimated features. However, similar to the model-based RME, the final results are sensitive to the selection of models. Moreover, traditional LDPL-based models are usually linear and cannot efficiently capture landscape information, e.g., building features. This motivated us to develop novel model-based features for RME.

To facilitate the radio propagation model with building information, we define a novel radio depth map to capture the surrounding information with physical models [3] as an additional input channel for the neural networks. Let N_t be the number of transmitters. The depth value in a radio depth map at location \mathbf{x}_i is defined as follows:

$$H(\mathbf{x}_i) = h(\sum_{i=1}^{N_t} E_j(\mathbf{x}_i) \cdot B_j(\mathbf{x}_i)), \tag{2}$$

where $E_j(\cdot)$ captures power from different transmitters defined by LPDL or IDW models, $B_j(\cdot)$ is calculated from the radiowave decay ratio over buildings considering the location of j-th transmitter, and $h(\cdot)$ is the normalization function. Instead of roughly defining PSD values, the radio depth map highlights the radio propagation model and the fading effect from buildings. We then utilize the radio depth map as the new input for a neural network. The results of one exemplary radiomap is shown in Fig. 4. Without suffering from overfitting the landscape in the urban map, results from radio depth map present a more accurate estimation on the radiomap patterns, leading to lower mean squared error (MSE) of the predicted received power compared to the traditional input features \mathcal{X} , thereby demonstrating the potential integration of the proposed

radio depth map and deep learning approaches in efficient RME. Here, we utilize MSE to evaluate the performance since it directly reflects the overall reconstruction accuracy. Other potential metrics also include the normalized MSE (NMSE) and the performance of outage map prediction derived from the estimated radiomap [4].

Discussion: This type of RME after physics-based processing provides flexibility to the design of learning framework. Different techniques, such as model-based interpolation or radio depth construction, can be used to extract features as the input of learning machines. From there, users can customize their neural networks design for estimation including deep convolutional neural networks and generative adversarial networks (GAN). Despite some demonstrated successes, selecting suitable models can still be intricate. Existing model-based feature extraction are usually LDPL-based. The specific customization, such as shadowing effects and channel fading, can improve performance and deserve further exploration.

B. Physics-Regularized Loss Function

Next, we introduce another type of physics-inspired machine learning based on physics-regularized loss function. Different from RME with physics-extracted features, these kind of methods still utilize the original features as input, while embedding the radio model information in the modified loss function. In general, the physics-regularized loss function can be formulated as

$$\min_{\Theta} L_1(\hat{R}(\mathcal{Z}_o), R(\mathcal{Z}_o)) + \alpha L_2(\hat{R}(\mathcal{Z})) + \lambda L_3(\hat{R}(\mathcal{Z}), \mathcal{P})$$
 (3)

where $\hat{R}(\mathcal{Z}) = g_{\Theta}(\mathcal{X}, R(\mathcal{Z}_o))$ is the mapping function (e.g. neural networks) with parameters Θ , and \mathcal{P} is the additional physics-based inputs.

Here, L_1 is the empirical loss to measure the quality of the approximation in the view of observed samples. Typical examples include the squared loss, absolute value loss, Huber loss and Log-Cosh loss, aiming to minimize the reconstructed error between $\hat{R}(\mathcal{Z}_o)$ and $R(\mathcal{Z}_o)$. Different designs of empirical loss may exhibit advantages for different datasets. For example, the squared loss can be differentiable everywhere, while the absolute loss might be less sensitive to the noise.

 L_2 is a regularization term, which could assist the optimization to capture a better geometric intuition and possess certain properties. One category of regularization terms consist of different norms, such as l_1 -norm, l_2 -norm, Frobenius norm and nuclear norm. These norms regularise the loss function during RME process. For example, the minimization on l_1 norm promotes sparsity of radiomap estimation, which may benefit the RME in the region with very low radio power. Another example is nuclear norm, which highlights signal properties in the singular domain and is widely used in RME based on tensor completion [13]. Another category of regularizers describes the geometric properties. A typical example is Laplacian regularizer, which favors the smoothness of the estimated radiomap.

Note that, the empirical loss L_1 and conventional regularizer L_2 mainly focus on properties of data, and rely on the quantity and quality of the training data. For example, as

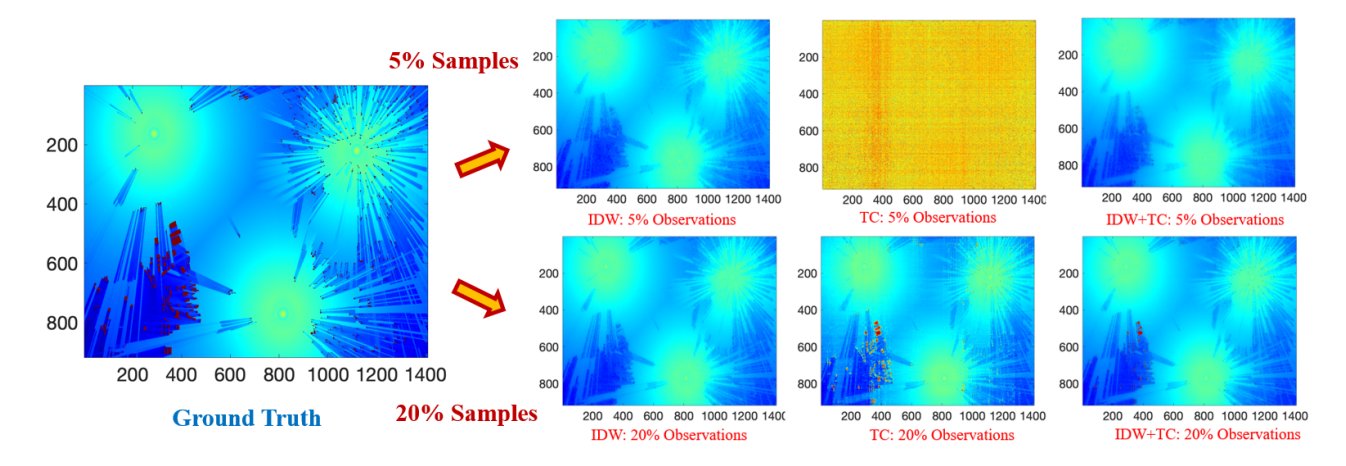


Fig. 5. Examples of RME with Different Loss Function: 1) IDW - purely model-based interpolation; 2) TC - conventional tensor completion; 3) IDW+TC - customized TC loss function integrated with model information (Buildings are marked as red).

shown in Fig. 5, model-based interpolation is able to capture the smooth patterns while failing to capture the detailed patterns near buildings. The tensor completion (TC) with conventional loss function needs more training samples to detect shadowing and obstacle effect compared to model-based interpolation. This observation motivates us to introduce a physics-inspired regularization term L_3 by integrating data statistics with physical radio models. One intuitive design of L_3 is first to estimate a radiomap based on MBI denoted by $\hat{R}_{k_{MBI}}$ and define the physics terms as $L_3(\hat{R}, \hat{R}_{k_{MBI}})$. For example, in [4], a conditional GAN is trained according to the cosine similarity of gradients for each location between \hat{R} and $R_{k_{MRI}}$ in L_3 to smooth the estimated radiomap. Another design is to minimize the weighted error between R and $R_{k_{MBI}}$ to restrict the optimization in the direction of LDPL propagation model. Shown in the first row in Fig. 5 with 5% observations, after embedding the IDW-based regularization term with conventional tensor completion loss, the IDW-TC succeeds in reconstructing the radiomap and overcomes failure of the TC-based method. Moreover, integrating the databased empirical and regularization loss with models, the IDW-TC method can model blocking and shadowing effects from landscape in comparison with IDW, as shown in the second row in Fig. 5. Other potential design of L_3 may also consider the segmentation of outage area, the intensity of radiomap pattern and the model-based pre-selected observations.

Discussion: Traditional data-driven and regularized loss functions may be limited by the quality and quantity of training samples. To address such challenges, learning with physics-regularized loss function can be an intuitive way to embed the model information to compensate for the low-fidelity of data samples. The key here is the effective design of L_3 and the adjustment of the weighting parameters, i.e., α and λ . To leverage the model information, model-based interpolation and physical radio propagation properties can be utilized to design the L_3 . Still, much work is needed to develop elegant integration to fit the datasets by considering channel noise, shadowing effects, and interference. Beyond the LDPL model, more accurate physical models, such as ray

tracing, uniform geometrical theory of diffraction or Maxwells equation solvers may be considered for RME in some specific small-scale scenarios. Equally important is the realization that various regions may have different degrees of model sensitivity, thereby motivating an adaptive weighting strategy for efficient RME. For example, the weight λ may depends on smoothness or regularity of the surrounding geographical features.

C. Learning with Physics-Guided Models

Beyond feature extraction and loss function design, we now consider customization of learning algorithms based on specific domain knowledge and model information, which was shown in Fig. 3.

We utilize model information to modify the conventional learning algorithms for specific tasks in RME. Here, we consider the RME for the restricted area as an example for illustration. As shown in Type-B in Fig. 2, RME for blank area aims to estimate PSD for the entire missing area, which is similar to the traditional image inpainting problem in computer vision [14]. Among a variety of image inpainting algorithms, exemplar-based image inpainting (EI) estimates missing values patch-by-patch from boundaries between observed regions and restricted regions, leading to the center of the restricted area. In this known efficient approach, the most important step is to determine the priority of the block to be filled and the direction of inpainting. Traditional EI methods favor the textures of images, where the inpainting direction shall follow the strength of isophotes hitting the boundary, defined by the gradient of texture s_p and the normal n_p at location **p** in the boundary. It is important to note that, unlike photographic images, radiomaps display clear patterns following the radio propagation from the transmitter. Thus, we integrate traditional image inpainting algorithms with physics-based models. Shown as Fig. 6, radio isophotes can be defined as the strength of the radio hitting the boundary between observed regions and missing regions. Different from traditional EI favoring the texture gradient, we define a radio texture term based on the radio propagation direction with a strength defined by the inverse distance or

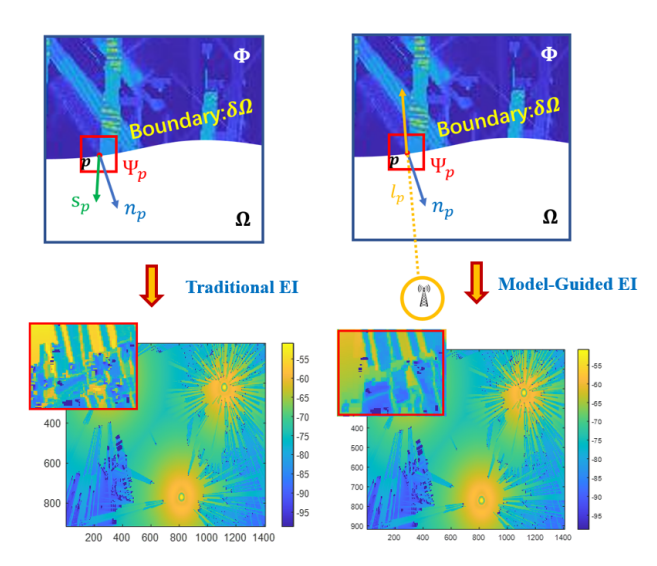


Fig. 6. Examples of RME of Restricted Areas: Traditional EI inpaints the missing area with texture gradients (MSE: 137.33); and Model-guided EI inpaints the missing area following the radio propagation model (MSE: 111.07).

LDPL models. Calculating the factors with the boundary norm, we could define a novel model-based priority and filling direction for image inpainting in radiomaps. The results are shown in Fig. 6, where the proposed model-guided algorithms can significantly improve the traditional image inpainting and dictionary learning approaches for radiomap estimation in restricted areas.

Beyond model-guided modification on the traditional learning algorithms for RME, another emerging technique is the physics-embedded neural network [11], which utilizes model information to guide the design and training process of neural networks. Usually, this kind of techniques formulate imaging or image reconstruction as a compressed sensing problem for estimating ϵ from $\Phi \epsilon$, where Φ is the sensing matrix based on the radio and geometry of the domain of investigation (DoI) embedding the model information. Deep learning networks based on unrolling have played an important role in solving such problems. A classic method is the iterative shrinkage thresholding algorithm (ISTA), which iteratively performs proximal gradient descent [15] to optimize ϵ . Despite the successes of unrolling in other applications, such as electromagnetic imaging and reconstruction, there have been very few related works in the domain of RME and reconstruction. Therefore, further research on the integration of the physicsembedded neural networks with RME is justified.

Discussion: Compared to physics-extracted features and physics-regularized loss function, learning algorithms guided by the physics models tend to be more complex but can perform better in specific applications [3]. Moreover, more efforts shall be contributed to the selection and design of suitable learning models that are amenable for integrating with radio propagation models.

IV. OPPORTUNITIES AND CHALLENGES

To further develop physics-inspired learning for RME and wireless communication applications, we address some opportunities and challenges in this field.

- Data Collection: For efficient implementation of machine learning algorithms, rich and large number of datasets play important roles. Existing datasets are mostly derived from software simulation, such as WinProp and Wireless *Insite*. One open dataset is RadioMapSeer Dataset¹ [8] generated from WinProp, which is frequency-sensitive. It consists of 700 maps, 80 transmitter locations per map, providing coarsely simulated radio maps in Europe. Another available data is the BRATLAB Dataset ² [3], which contains WinProp-simulated radiomaps for both single-band and multi-band scenarios, covering several US cities. Different from RadioMapSeer dataset, BRAT-LAB Dataset includes both coarse and fine resolution radiomaps. In addition, Johns Hopkins University Applied Physics Laboratory (JHU-APL) provided a dataset simulated from Wireless inSite with 1-meter resolution Light Detection and Ranging (LIDAR) information of a select region in Atlanta, Georgia, USA [3]. This highfidelity simulated JHU-APL dataset includes shadowing and obstacle effects. Despite the success of synthetic datasets, easier access to real-life datasets collected by sensors could improve radio propagation modeling and further assist RME algorithm development. In addition, data generation from synthetic samples and realistic measurements based on the emerging generative learning models can be another promising direction. Another shortcoming is that most datasets focus on the 2D spatial geometry, whereas 3D radiomap is also of great interest, especially for UAV deployment. There is an acute need for, and plenty of opportunities in, acquiring multi-band higher resolution radio coverage information in 2D/3D.
- Radio Model Physics: Incorporating physics theory into data-driven methods is challenging. A general model can strengthen the robustness of physics-inspired RME, whereas a specified physics model can lead to accurate RME in a given scenario. The selection of a suitable model is important for all three types of physics-inspired machine learning algorithms we have discussed. Beyond radio propagation models, there is also a strong need for better interference models and channel fading models to provide a more accurate description of the radiomaps.
- Down-Stream Applications: Rapid growth and broad deployment of IoT and 5G systems make efficient estimation and utilization of radiomaps increasingly important. Radiomap estimation is a valuable tool in resource allocation and network planning of future wireless communication systems. One promising direction is radiomap-based localization and footprinting. Evaluating spectral distribution from estimated radiomaps, efficient approaches can be designed for traditional wireless localization. Another direction can be the end-to-end learning frameworks of spectrum/power management and network optimization. With RME, one may develop end-to-end data-driven approaches for specific network applications, such as

¹https://radiomapseer.github.io/

²https://github.com/BRATLab-UCD/Radiomap-Data

outage detection, fault diagnosis and wireless spectrum planning. Other practical directions include radiomap based interference estimation across different bands and regions, as well as dynamic radiomap prediction.

V. CONCLUSION

This article provides an overview of physics-inspired machine learning for radiomap estimation based on integrating real-time measurement data with physical properties of radio propagation. Specifically, we introduce three different types of physics-inspired RME: 1) learning with physics-extracted features; 2) learning with physics-regularized loss functions; and 3) learning guided by physics models. Fundamentally, the incorporation of physics models facilitates the machine learning with ability to uncover the hidden PSD distribution more efficiently, even without high quality or dense data samples. The development of efficient and accurate RME solutions, can lead to extensive applications such as interference management, spectrum resource allocation, UAV path planning and outage detection. With the development of artificial intelligence and its integration within wireless networking, efficient physics-inspired RMEs are expected to generate more accurate and valuable radiomaps to significantly benefit future wireless communication networks.

VI. ACKNOWLEDGEMENT

This material is based upon works supported in part by University of Louisiana at Lafayette Research Fund; and in part by the National Science Foundation under Grant 2029027 and Grant 2332760; and in part by Johns Hopkins University Applied Physics Internal Research and Development funds.

REFERENCES

- D. Romero and S.-J. Kim, "Radio map estimation: a data-driven approach to spectrum cartography," in *IEEE Signal Processing Magazine*, vol. 39, no. 6, pp. 53-72, Nov. 2022
- [2] S. Bi, J. Lyu, Z. Ding and R. Zhang, "Engineering Radio Maps for Wireless Resource Management," in *IEEE Wireless Communications*, vol. 26, no. 2, pp. 133-141, Apr. 2019.
- [3] S. Zhang, T. Yu, B. Choi, F. Ouyang, and Z. Ding, "Radiomap inpainting for restricted areas based on propagation priority and depth map," in *IEEE Transactions on Wireless Communications*, Feb. 2024.
- [4] S. Zhang, A. Wijesinghe and Z. Ding, "Rme-gan: a learning framework for radio map estimation based on conditional generative adversarial network," in *IEEE Internet of Things Journal*, May 2023.
- [5] W. A. Hapsari, A. Umesh, M. Iwamura, M. Tomala, B. Gyula and B. Sebire, "Minimization of drive tests solution in 3GPP," in *IEEE Communications Magazine*, vol. 50, no. 6, pp. 28-36, Jun. 2012.
- [6] M. Lee and D. Han, "Voronoi tessellation based interpolation method for wi-fi radio map construction," in *IEEE Communications Letters*, vol. 16, no. 3, pp. 404-407, Mar. 2012.
- [7] S. -P. Kuo and Y. -C. Tseng, "Discriminant minimization search for large-scale rf-based localization systems," in *IEEE Transactions on Mobile Computing*, vol. 10, no. 2, pp. 291-304, Feb. 2011.
- [8] R. Levie, Ç. Yapar, G. Kutyniok and G. Caire, "Radiounet: fast radio map estimation with convolutional neural networks," in *IEEE Transactions on Wireless Communications*, vol. 20, no. 6, pp. 4001-4015, Jun. 2021.
- [9] Y. Teganya and D. Romero, "Deep completion autoencoders for radio map estimation," in *IEEE Transactions on Wireless Communications*, vol. 21, no. 3, pp. 1710-1724, Mar. 2022.
- [10] Y. Zheng, J. Wang, X. Li, J. Li and S. Liu, "Cell-Level RSRP Estimation With the Image-to-Image Wireless Propagation Model Based on Measured Data," in *IEEE Transactions on Cognitive Communications and Networking*, vol. 9, no. 6, pp. 1412-1423, Dec. 2023.

- [11] R. Guo, T. Huang, M. Li, H. Zhang and Y. C. Eldar, "Physics-embedded machine learning for electromagnetic data imaging: examining three types of data-driven imaging methods," in *IEEE Signal Processing Magazine*, vol. 40, no. 2, pp. 18-31, Mar. 2023.
- [12] A. Creswell, T. White, V. Dumoulin, K. Arulkumaran, B. Sengupta and A. A. Bharath, "Generative adversarial networks: an overview," in *IEEE Signal Processing Magazine*, vol. 35, no. 1, pp. 53-65, Jan. 2018.
- [13] D. Schäufele, R. L. G. Cavalcante and S. Stanczak, "Tensor completion for radio map reconstruction using low rank and smoothness," 2019 IEEE 20th International Workshop on Signal Processing Advances in Wireless Communications (SPAWC), Cannes, France, 2019, pp. 1-5.
- [14] A. Criminisi, P. Perez and K. Toyama, "Region filling and object removal by exemplar-based image inpainting," in *IEEE Transactions on Image Processing*, vol. 13, no. 9, pp. 1200-1212, Sep. 2004.
- [15] A. Beck and M. Teboulle, "A fast iterative shrinkage-thresholding algorithm for linear inverse problems," SIAM J. Imag. Sci., vol. 2, no. 1, pp. 183–202, Mar. 2009.

BIOGRAPHY

Songyang Zhang [M] received the Ph.D. degree in Department of Electrical and Computer Engineering from the University of California at Davis, Davis, CA, USA, in 2021, where he was a Postdoctoral Research Associate from August 2021 to July 2023. He is currently an Assistant Professor with the Department of Electrical and Computer Engineering in University of Louisiana at Lafayette, Lafayette, LA, USA. His current research interests include machine learning, signal processing, IoT intelligence and wireless communication. He received the Best Paper Finalist in the 2020 IEEE International Conference on Image Processing, and was recognized as the Best TCSVT Reviewer of 2022 by IEEE Circuits and System Society.

Brian Choi [SM] received his Ph.D. degree in Electrical and Computer Engineering from Virginia Tech in 2012. He is currently a member of the senior professional staff at The Johns Hopkins University Applied Physics Laboratory (JHU/APL) and a faculty member of Engineering for Professionals (EP) at The Johns Hopkins University. Before joining JHU/APL, he has worked as a graduate intern at the U.S. Air Force Research Laboratory (ARFL) and also at the Joint Spectrum Center (JSC). He has been working in the area of communication systems for over 15 years since his M.S. at University at Buffalo and his current research interests include military communications and waveforms, spectrum sharing, distributed systems and wireless sensor networks. He holds his B.S. in Electrical Engineering from Seoul National University. Dr. Choi is a senior member of IEEE.

Feng Ouyang [SM] earned his Master and Ph.D. degrees from Cornell University. He is currently a member of the senior professional staff at Johns Hopkins University Applied Physics Laboratory. His research areas include commercial wireless communications, communication security, and directional wireless networks.

Zhi Ding [F] holds the position of distinguished professor in the Department of Electrical and Computer Engineering at the University of California, Davis. He received his Ph.D. degree from Cornell University in 1990. His major research interests cover wireless networking, signal processing, multimedia, and learning. Prof. Ding is a Fellow of IEEE. He served as associate editor for IEEE Transactions on Signal Processing from 1994-1997, 2001-2004, and for IEEE Signal Processing Letters 2002-2005. Dr. Ding was the General Chair of the 2016 IEEE International Conference on Acoustics, Speech, and Signal Processing and the Technical Program Chair of the 2006 IEEE Globecom. Dr. Ding is a coauthor of the textbook: Modern Digital and Analog Communication Systems, 5 th edition, Oxford University Press, 2019. Prof. Ding received the IEEE Communication Society's WTC Award in 2012 and the IEEE Communication Society's Education Award in 2020.